



Investigation of the Passivation and Semiconducting Behavior of Alloy C (UNS N10002) in HNO₃ Solutions

Arash Fattah-Alhosseini*, Azam Khodabandeloie, Mahsa Bahirae
Department of Materials Engineering, Bu-Ali Sina University, Hamedan 65178-38695, Iran

Received 27 Feb 2015, Revised 21 Jul 2015, Accepted 24 Jul 2015

*Corresponding author: E-mail: a.fattah@basu.ac.ir; Tel: (+988138292509)

Abstract

This study focuses on the passivation and semiconducting behavior of alloy C in HNO₃ solutions. The report includes potentiodynamic polarization and electrochemical impedance spectroscopy (EIS) studies along with Mott-Schottky analysis in order to determine the passive behavior of the alloy and the semiconducting properties of the passive film formed during exposure to acidic solutions. Mott-Schottky plots indicated that the donor densities increase with decreasing HNO₃ concentration. Moreover, more positive values of the flat band potential indicate better stability of the passive film with decreasing HNO₃ concentration. EIS measurements showed that the reciprocal capacitance (1/C) of the passive film is directly proportional to its thickness which increases with decreasing HNO₃ concentration. Therefore, it is clear that dilute HNO₃ solutions offer better conditions for forming the passive films with higher protection behavior, due to the growth of a much thicker and more defective passive films.

Keywords: Alloy C; Polarization: EIS; Mott-Schottky plot; Passive film.

Introduction

Chromium-containing Ni-base alloys have excellent passivation and electrochemical behavior in aggressive acidic and basic solutions, which are attributed to the ability of nickel and chromium to form a stable passive film [1–3]. The mentioned behavior is correlated to the formation of the passive film whose compositional and electrochemical properties have been studied using surface analytical and electrochemical methods [2–17].

Recently, the variation in chemical composition of the passive films has been studied using X-ray photoelectron spectroscopy (XPS) and secondary ion mass spectrometry. Latest studies showed that the chemical composition of the passive films formed on Ni-base alloys depends on many variables such as pH, presence of aggressive anions, and aerating conditions [18–21]. Lloyd et al. [9–11] investigated the chemical composition and thickness of the passive films formed on a number of Ni-base alloys in acidic solution. Moreover, they studied the effect of the main alloying elements (Cr, Mo and W) on the passivity of these alloys in acidic solution. The results showed that the passive films thickness increase with increasing potential in the passive region. Also, the results indicated that the passive films consist of a Mo, Cr, Ni oxide, with Cr present as Cr (III) and Mo in several oxidation states [9–11].

Moreover, the variation in electrochemical properties of the passive films has been investigated using EIS and other electrochemical measurements. Priyantha et al. [14] studied the passive film properties on alloy C-22 in NaCl brine at elevated temperature by EIS over the potential range from -0.2 to 0.7 V_{Ag/AgCl}. Jakupi et al. [22] investigated the passive film properties on alloy C-22 in near neutral pH, 5 M NaCl solutions by EIS.

Generally, there are many industrial processes in which the Ni-base alloys (especially alloy C) have to withstand the acidic solutions and these solutions can affect the passivation and electrochemical behavior of these alloys. However, little information about the passivation and semiconducting behavior of the alloy C (UNS N10002) in the acidic solutions was available. The aim of this study is to investigate the electrochemical behavior of alloy C in HNO₃ solutions by using the EIS and Mott-Schottky analysis. Also, this work includes determination of the semiconductor character and estimation of the dopant levels in the passive film, as well as the investigation of the impedance behavior as a function of HNO₃ concentration.

2. Materials and methods

Specimens were fabricated from Alloy C (UNS N10002) with the chemical composition (% , wt.): 54.4 Ni, 14.3 Cr, 17.4 Mo, 5.14 Fe, 4.15 W, 2.12 Co, 1.53 Cu, 0.406 Mn, 0.005 Si, 0.128 V, and 0.01 C. All samples were polished mechanically by abrading with wet emery paper up to 1200 grit size and then dried with air just before each the electrochemical measurements. The acidic solutions with five different concentrations (2.0, 1.0, 0.5, 0.1 and 0.01 M HNO₃) were used as the test solutions at 25±1 °C.

All the electrochemical measurements were performed in a conventional three-electrode flat cell under aerated conditions. The counter electrode was a Pt plate, while the reference electrode was Ag/AgCl saturated in KCl. The electrochemical measurements were obtained by using an Autolab potentiostat/galvanostat system. Prior to the electrochemical measurements, the working electrodes were immersed at open circuit potential (OCP) to form a steady-state passive film.

The potentiodynamic polarization curves were measured potentiodynamically at a scan rate of 1 mV/s starting from -0.25 V_{Ag/AgCl} (vs. E_{corr}) to 1.0 V_{Ag/AgCl}. The impedance spectra were measured in a frequency range of 100 kHz -10 mHz at an AC amplitude of 10 mV (rms). For the EIS data modeling and curve-fitting method, the NOVA impedance software was used. The Mott-Schottky analysis were carried out on the passive films at a frequency of 1 kHz using a 10 mV ac signal, and a step rate of 25 mV in the cathodic direction.

3. Results and discussion

3.1. Polarization measurements

The potentiodynamic polarization curves of alloy C in HNO₃ solutions is shown in Fig. 1. As expected, the alloy C showed excellent passive behavior. It is observed that all curves exhibit similar features, with a passive potential range extending from the corrosion potential to the onset of transpassivity. By comparing the curves in different solutions, the current density was found to increase with potential during the early stage of passivation and no obvious current peak was observed.

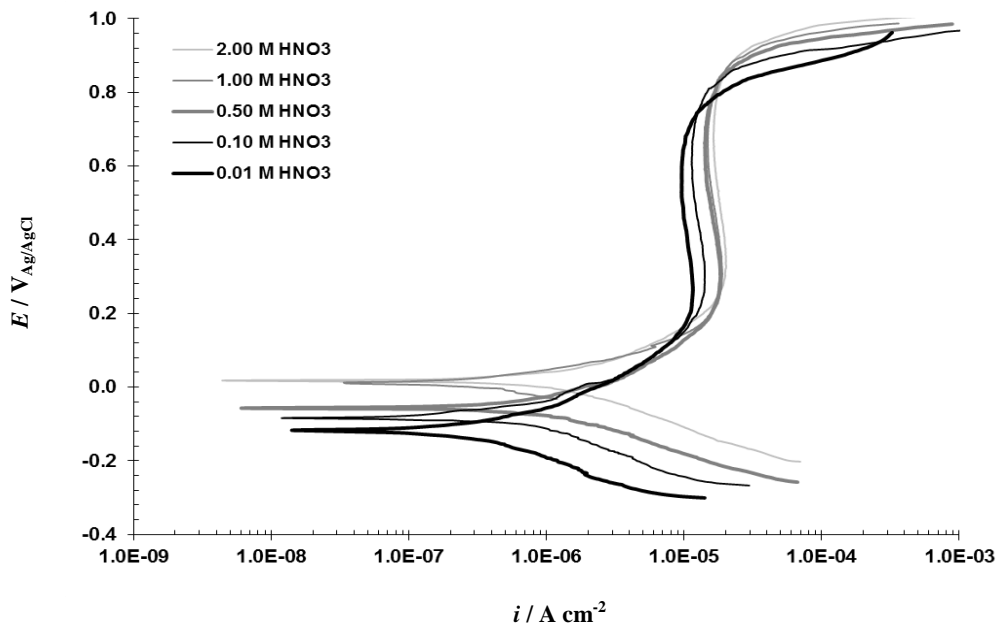


Figure 1: Potentiodynamic polarization curves of alloy C in HNO₃ solutions.

The variation of the corrosion and breakdown potentials of alloy C in HNO₃ solutions are illustrated in Fig. 2. It is observed that both potentials shift towards the negative value with decrease in solution concentration. Generally, Tafel extrapolation method is widely used for the measurement of the corrosion rate. By this method, the corrosion current density (*i*_{corr}) was calculated of the linear part for the cathodic branch back to the corrosion potential [23]. Fig. 3 shows the effect of the concentration of HNO₃ solutions on the corrosion current density of alloy C. It is obvious the corrosion current density decreases with decrease in the concentration of HNO₃ solutions.

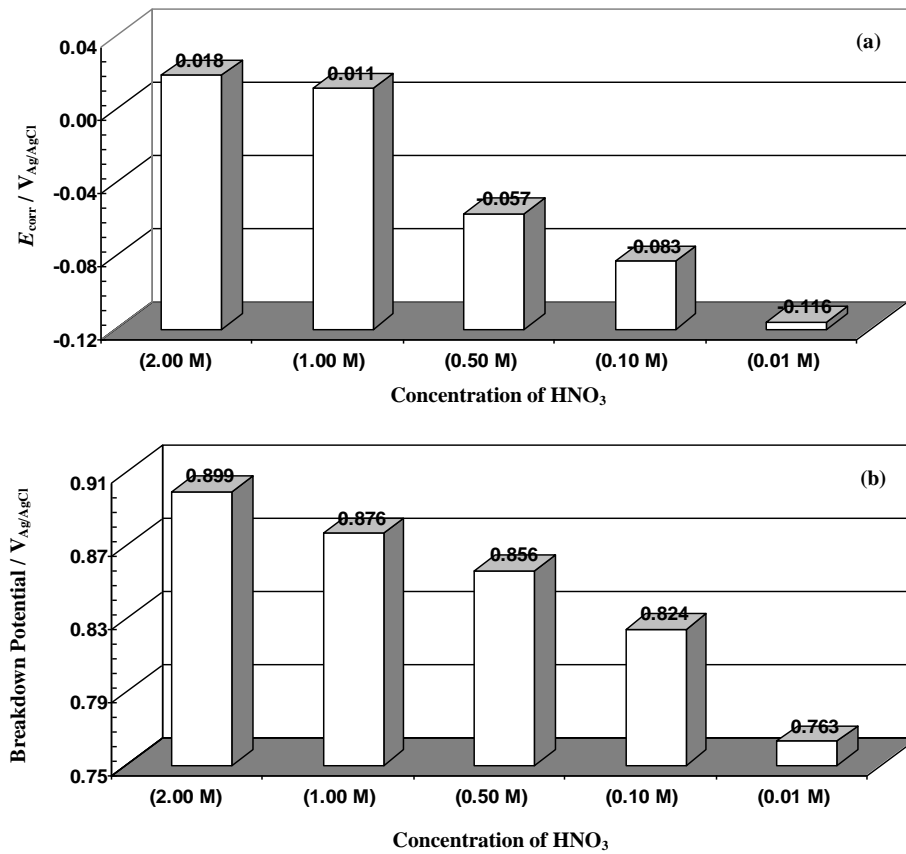


Figure 2: Variation of the (a) corrosion and (b) breakdown potentials of alloy C in HNO₃ solutions.

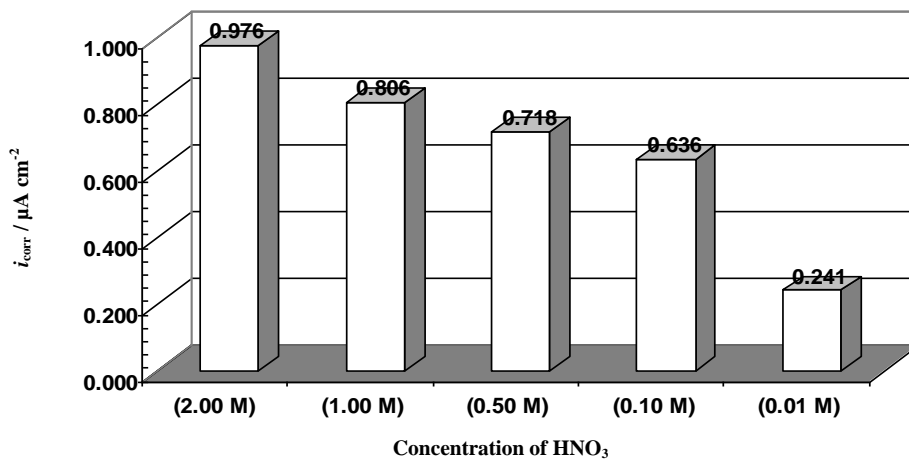


Figure 3: Variation of the corrosion current density of alloy C in HNO₃ solutions.

3.2. Mott-Schottky analysis

Based on the Mott-Schottky analysis, the potential dependence of the space-charge layer capacitance (C_{sc}) given by the following the Mott-Schottky relationships assuming that the capacitance of the Helmholtz layer could be neglected [23–25]:

$$\frac{1}{C_{sc}^2} = \frac{2}{\epsilon \epsilon_0 e N_D} \left(E - E_{FB} - \frac{k_B T}{q} \right) \quad (1)$$

where e is the electron charge, N_D represents the donor density for n-type semiconductors (cm^{-3}), ϵ stands for the dielectric constant of the passive film (usually taken as 20 for alloys 22 [3, 25]), ϵ_0 denotes the vacuum permittivity, k , T , and E_{fb} are the Boltzmann constant, absolute temperature, and flat band potential, respectively.

The semiconductor type can be distinguished according to the positive or negative slope (positive slope indicates n-type, whereas the negative indicates p-type). Fig. 4 shows the Mott-Schottky plots of alloy C in HNO_3 solutions. It should be noted that capacitances clearly increase with solution concentration. Moreover, a linear relationship between C^{-2} and E can be observed. The positive slopes in the potential range of around -0.1 – $0.4 \text{ V}_{\text{Ag}/\text{AgCl}}$ are attributed to an n-type behavior. At potentials higher than $0.4 \text{ V}_{\text{Ag}/\text{AgCl}}$, the appearance of a peak in Mott-Schottky plots indicates an inversion from n-type to p-type semiconductor. Similar Mott-Schottky plots for alloy 22 in $0.5 \text{ M H}_2\text{SO}_4$ solution have been reported by Raja et al. [3]. In these plots, more positive values of flat band potential indicate better stability of the passive film with decreasing HNO_3 concentration.

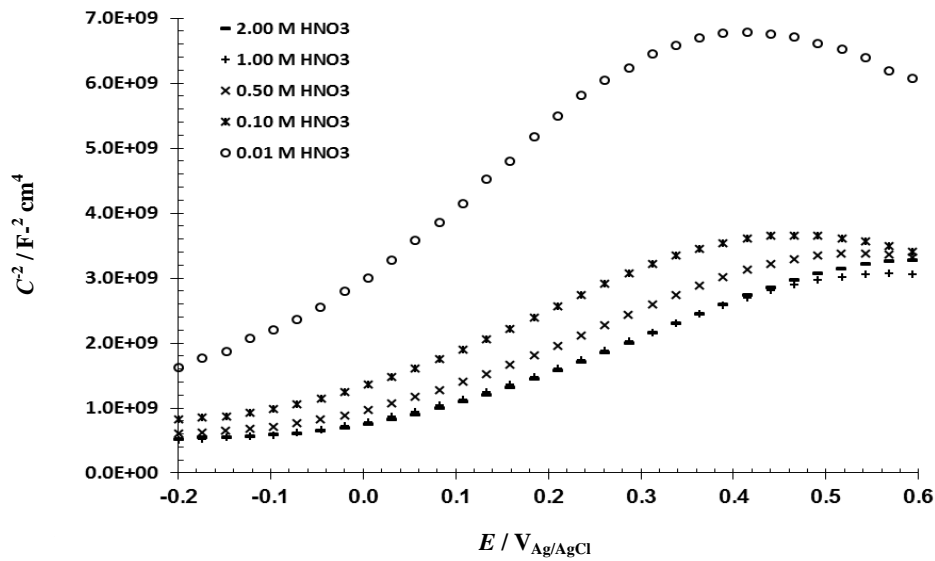


Figure 4: Mott-Schottky plots of alloy C in HNO_3 solutions.

According to Eq. (1), the donor density (N_D) can be calculated from the slope of the experimental $1/C^2$ versus E plots. Fig. 5 shows the calculated donor density of alloy C in HNO_3 solutions. In these solutions, only donor densities are calculated because predominantly n-type behavior could be observed from the Mott-Schottky plots. According to Fig. 5, the donor densities are in the order of 10^{21} cm^{-3} and increase with decreasing HNO_3 concentration.

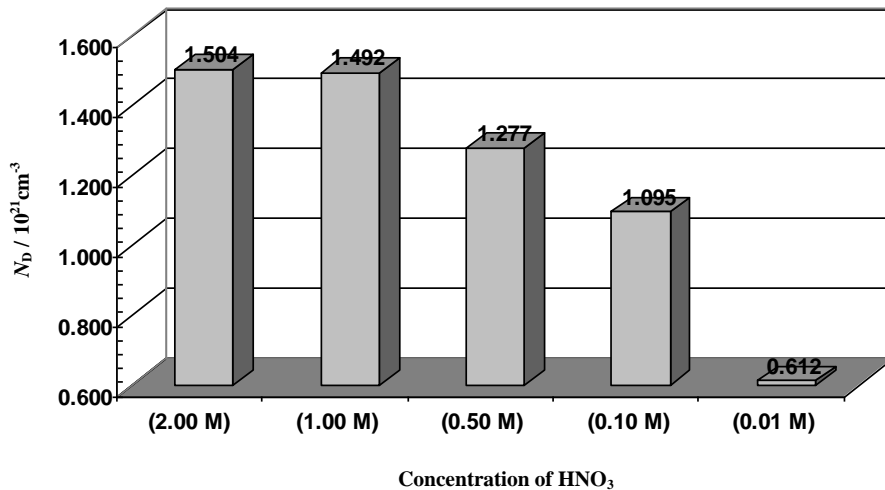


Figure 5: Calculated donor density of the passive films formed on alloy C in HNO_3 solutions.

Similar values for the donor densities (10^{21} cm^{-3}) have been reported for alloy 22 in 0.5 M H_2SO_4 solution [3]. Indeed, the changes in the donor density related to the non-stoichiometry defects in the passive films. Based on the point defect model [29-31], the flux of oxygen vacancy and/or cation interstitials through the passive film is essential to the film growth process. In this concept, the dominant point defects in the passive film are considered to be oxygen vacancies and/or cation interstitials acting as electron donors. It is mentioned that in the potential range of around -0.1 – $-0.4 \text{ V}_{\text{Ag}/\text{AgCl}}$ no evidence for p-type behavior was obtained, indicating that cation vacancies do not have any significant population density in the passive film.

3.3. EIS measurements

The EIS response of alloy C in HNO_3 solutions was done at the steady-state corrosion potential and the results are shown as Nyquist and Bode plots in Fig. 6.

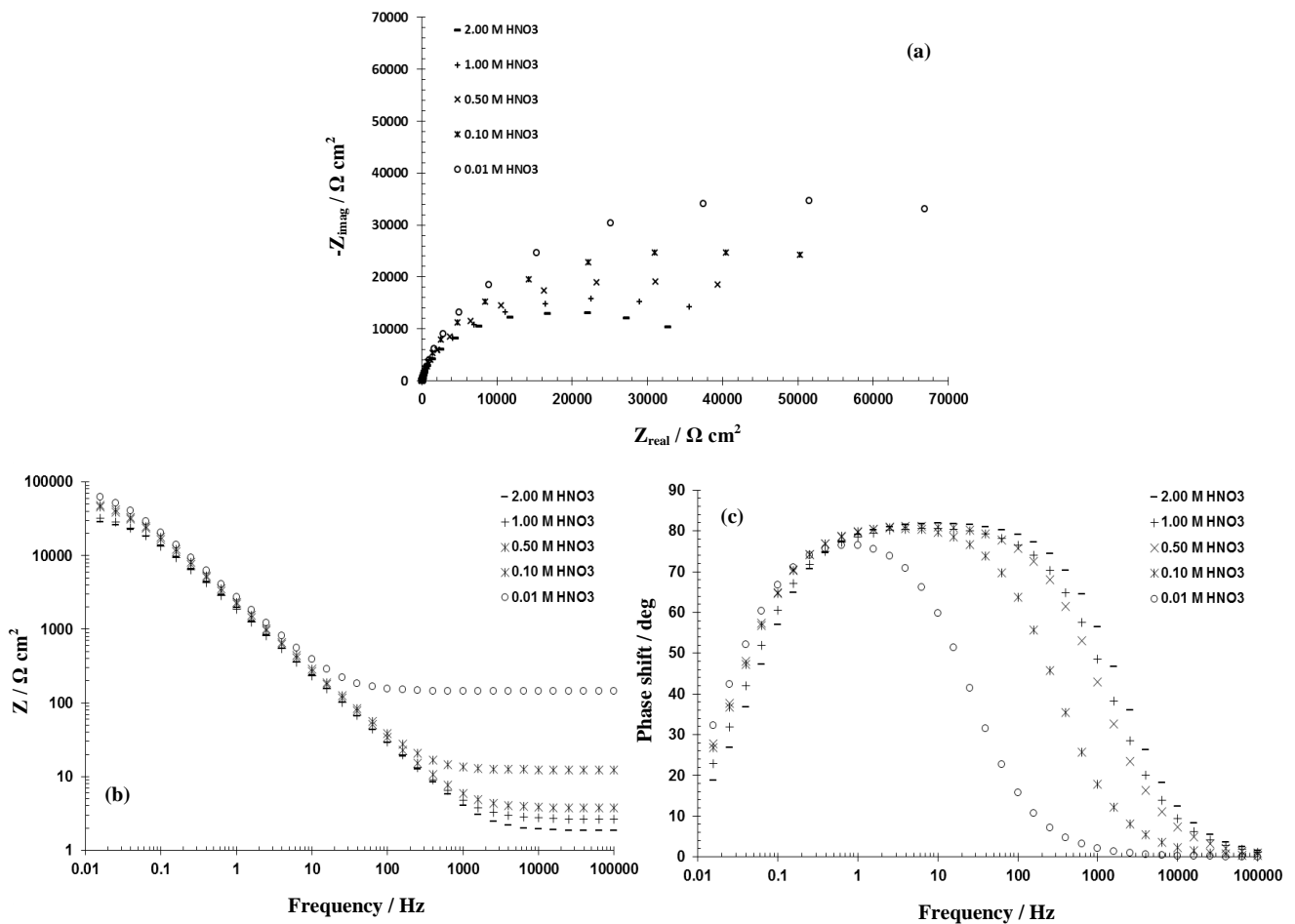


Figure 6: (a) Nyquist, (b) Bode, and (c) Bode-phase plots of alloy C in HNO_3 solutions.

The Nyquist and Bode plots show a resistive behavior at high frequencies, but in the middle to low frequency range there was a marked capacitive response. The Bode-phase curves show one time constant (only one maximum phase lag at the middle frequency range). The phase angles values remained very close to 90° . This evolution revealed the formation and growth of a passive film [23]. Also, there was a decrease of the low frequency impedance with the solution concentration. Indeed, the capacitive impedance is the least in 2.0 M HNO_3 solution and increases with dilution. Based on these results, the equivalent circuit shown in Fig. 7 was used to simulate the measured impedance data on alloy C in HNO_3 solutions. This equivalent circuit is composed of: R_s – solution resistance; Q_{pf} – constant phase element corresponding to the capacitance of the passive film; R_{pf} – resistance of the passive film [2].

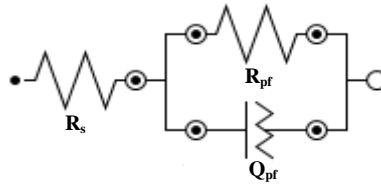


Figure 7: The best equivalent circuit used to model the experimental EIS data [2, 3].

The variation of the resistance and capacitance of the passive films formed on alloy C in HNO₃ solutions are illustrated in Fig. 8 (a) and (b), respectively.

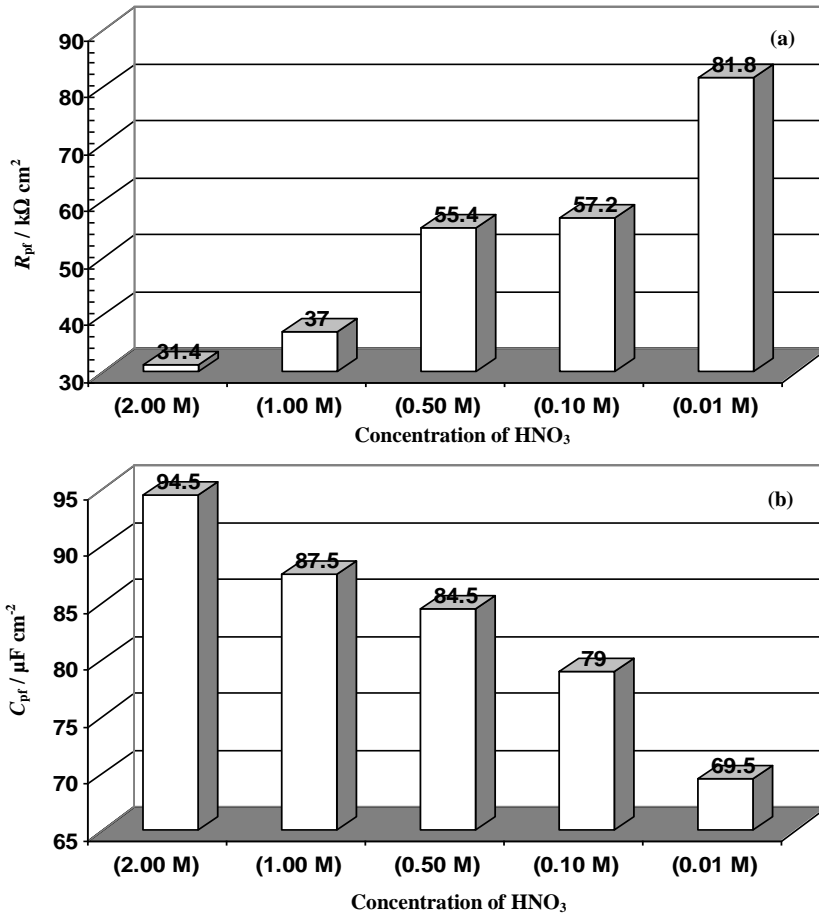


Figure 8: Variation of the (a) resistance and (b) capacitance of the passive films formed on alloy C in HNO₃ solutions.

As can be seen, R_{pf} increases with decrease in HNO₃ concentration while C decreases. This behavior indicates that grown passive film on alloy C surface is liable to dissolve in high HNO₃ concentration, since R_{pf} is inversely proportional to the corrosion current density [23]. Based on the equivalent circuit shown in Fig. 7, the passive film thickness (d) can be determined by the Eq. (2) [2]:

$$d = \frac{\epsilon_0 A}{C} \tag{2}$$

where C is the total capacitance of the passive film, and A the area in cm². Indeed, a change in the total capacitance of the passive film (C) can be used as an indicator for change in the passive film thickness (d). Therefore, the reciprocal capacitance of the passive film ($1/C$) is proportional to its thickness which increases with decreasing HNO₃ concentration. It is clear that dilute HNO₃ solutions give better conditions for forming the passive films with higher protection behavior, due to the growth of a much thicker and more defective passive films.

Conclusion

The electrochemical behavior of alloy C in HNO₃ solutions were investigated in the present work. Conclusions drawn from the study are as follows

1. Potentiodynamic polarization curves showed that alloy C showed excellent passive behavior in HNO₃ solutions.
2. No evidence of p-type semiconducting behavior was found in the Mott–Schottky analysis, indicating that the oxygen vacancies and interstitials preponderated over the cation vacancies.
3. Also, the Mott–Schottky analysis showed that the donor densities are in the order of 10²¹ cm⁻³, which increase with decreasing HNO₃ concentration.
4. EIS results showed that the reciprocal capacitance of the passive film is directly proportional to its thickness which increases with decreasing HNO₃ concentration.
5. Also, EIS results showed that dilute HNO₃ solutions offer better conditions for forming passive films with higher protection behavior, due to the growth of a much thicker and more defective films.

References

1. Fattah-alhosseini A., *Arab. J. Sci. Eng.* 40 (2015) 63.
2. Gray J.J., El Dasher B.S., Orme C.A., *Sur. Sci.* 600 (2006) 2488.
3. Raja K.S., Namjoshi S.A., Misra M., *Mater. Lett.* 59 (2005) 570.
4. Gray J.J., Hayes J.R., Gdowski G.E., Viani B.E., Orme C.A., *J. Electrochem. Soc.* 153 (3) (2006) B61.
5. Gray J.J., Hayes J.R., Gdowski G.E., Orme C.A., *J. Electrochem. Soc.* 153 (5) (2006) B156.
6. Macdonald D.D., *Electrochim. Acta*, 56 (2011) 7411.
7. Rodríguez M.A., Carranza R.M., Rebak R.B., *J. Electrochem. Soc.* 157 (1) (2010) C1.
8. Rybalka K.V., Beketaeva L.A., Davydov A.D., *Corros. Sci.* 54 (2012) 161.
9. Lloyd A.C., Shoesmith D.W., McIntyre N.S., Noel J.J., *J. Electrochem. Soc.* 150 (2003) B120.
10. Lloyd A.C., Noel J.J., McIntyre N.S., Shoesmith D.W., *JOM* 57 (2005) 31.
11. Lloyd A.C., Noel J.J., McIntyre N.S., Shoesmith D.W., *Electrochim. Acta* 49 (2004) 3015.
12. Andresen P.L., Young L.M., Catlin G.M., Emigh P.W., Gordon G.M., *Metall. Mater. Trans. A* 36 (2005) 1187.
13. Macdonald D.D., Sun A., Priyantha N., Jayaweera P., *J. Electroanal. Chem.* 572 (2004) 421.
14. Priyantha N., Jayaweera P., Macdonald D.D., Sun A., *J. Electroanal. Chem.* 572 (2004) 409
15. Bojinov M., Galtayries A., Kinnunen P., Machet A., Marcus P., *Electrochim. Acta* 52 (2007) 7475.
16. Macdonald D.D., Sun A., *Electrochim. Acta* 51 (2006) 1767.
17. Bojinov M., Kinnunen P., Sundholm G., *Corrosion* 59 (2003) 91.
18. Rodríguez M.A., Carranza R.M., Rebak R.B., *Metall. Mater. Trans. A* 36A (5) (2005) 1179.
19. Zhang X., Shoesmith D.W., *Corros. Sci.* 76 (2013) 424.
20. X. Zhang, D. Zagidulin, D.W. Shoesmith, *Electrochim. Acta* 89 (2013) 814.
21. Zagidulin D., Zhang X., Zhou J., Noël J.J., Shoesmith D.W., *Surf. Interf. Anal.* 45 (2013) 1014.
22. Jakupi P., Zagidulin D., Noël J.J., Shoesmith D.W., *Electrochim. Acta* 56 (2011) 6251.
23. Fattah-alhosseini A., Sabaghi Joni M., *J. Magnes. Allo.* 2 (2014) 175
24. Sikora E., Macdonald D.D., *Electrochim. Acta*, 48 (2002) 69.
25. Bellanger G., Rameau J.J., *J. Mater. Sci.* 31 (1996) 2097.
26. Zhang L., Macdonald D.D., *Electrochim. Acta* 43 (1998) 2661.
27. Zhang L., Macdonald D.D., *Electrochim. Acta* 43 (1998) 2673.
28. Nishimura R., *Corrosion*. 43 (1987) 486.
29. Macdonald D.D., *J. Electrochem. Soc.* 153 (2006) B213.
30. Macdonald D.D., *J. Nuclear Mater.* 379 (2008) 24.
31. Macdonald D.D., Urquidi-Macdonald M., *J. Electrochem. Soc.* 137 (1990) 2395.

(2016) ; <http://www.jmaterenvironsci.com>